



Low Expression of A3C and PLP2 Indicating a Favorable Prognosis in Human Gliomas

Jong-Shiaw Jin^{1#}, Yu-Ling Tsai^{2#}, Yu-Chan Chang³, Wen-Chiuan Tsai^{2,4*}

¹ Department of Pathology, Tungs' Taichung MetroHarbor Hospital, Taichung 40435, Taiwan

² Department of Pathology, Tri-Service General Hospital, National Defense Medical Center, Taipei 11490, Taiwan

³ Department of Biomedical Imaging and Radiological Sciences, National Yang Ming Chiao Tung University, Taipei, Taiwan

⁴ Graduate Institute of Pathology and Parasitology, National Defense Medical Center, Taipei, Taiwan, R.O.C

[#]These authors contributed equally to the research.

ARTICLE INFO

Original paper

Article history:

Received: April 09, 2023

Accepted: May 24, 2023

Published: July 31, 2023

Keywords:

Glioma, APOBEC3C, PLP2, immunostaining scores, prognosis

ABSTRACT

The roles of apolipoprotein B mRNA-editing enzyme catalytic polypeptide-like 3C (A3C) in various human malignancies are not consistent. A3C expression is correlated with early-stage breast cancer and is presented as a good prognostic factor; however, it induces fewer therapeutic effects of cytotoxic drugs in low-grade gliomas. To explore the impact of A3C on gliomas, a statistical analysis of several public databases was conducted. The results showed that enhanced A3C expression was associated with advanced tumor grades and poor expression of prognostic factors. Similarly, our *in vitro* study revealed that glioblastoma (GBM) cell lines had higher A3C mRNA and protein expression than that of normal brain tissue cDNA and lysates. We first performed an immunohistochemical stain (IHC) to prove that gliomas with high A3C expression presented the wild type-Isocitrate dehydrogenase 1 (IDH1), and they had an unfavorable prognosis in human glioma tissues. In addition, the oncological factors associated with A3C expression suggested that DNA repair pathways are important mechanisms for inducing tumorigenesis and chemoresistance in gliomas. Moreover, a significant correlation was observed between A3C expression and proteolipid protein 2 (PLP2). Reactive oxygen species (ROS) -activated PLP2 prevents DNA damage-induced cell apoptosis. Compared to high immunostaining scores for A3C and/or PLP2 expression, combined low immunostaining scores for A3C and PLP2 correlated with improved survival in gliomas; however, the detailed mechanism is to be elucidated. In conclusion, our results not only confirmed A3C played an important role in glioma development, but the A3C IHC test could successfully predict the therapeutic effects and disease prognosis.

Doi: <http://dx.doi.org/10.14715/cmb/2023.69.7.12>

Copyright: © 2023 by the C.M.B. Association. All rights reserved.

Introduction

Gliomas, originating from glial cells, are the most common primary tumors of the central nervous system (CNS) (1,2). Although the median age of patients with glioma is >60 years, primary brain tumors are the secondary malignant neoplasm of children of age ≤14 years (3). In a previous study, histological tumor grading was revealed to be highly relevant to the therapeutic policy; however, the discordance between histological appearances and therapeutic results was a major challenge for prognosis. According to the 2016 World Health Organization (WHO) classification of CNS tumors, molecular analysis is an important tool for the precise diagnosis and the development of a convenient and targeted therapeutic regimen (4). IDH1/2 mutations, 1p19q chromosomal co-deletion, alpha-thalassemia x-linked mental retardation (ATRX), and TP53 mutations are critical for evaluating aggressive glioma behavior (5). The p53, mitogen-activated protein kinase/extracellular signal-related kinase (MAPK/ERK), and retinoblastoma (RB) are the major pathways associated with glioma progression and invasion (6). Temozolomide (TMZ), the standard treatment for DNA breakage in

high-grade gliomas, inhibits tumor survival (7). However, O⁶-methylguanine-DNA methyltransferase (MGMT) and poly [ADP-ribose] polymerase 1 (PARP-1) induce therapeutic failure during systemic chemotherapy or radiotherapy by repairing the damaged DNA sites (7,8). A3C was discovered as a nucleolar protein located at the DNA damage site stimulated by genotoxic ROS (9). Based on a review of several human cancer databases, Luo *et al* (10) demonstrated that an A3C mutation resulted in tumor progression and poor prognosis of gliomas.

ROS is produced by NADPH-dependent uncoupled electron transduction and induces free radical activation, thereby modulating the cell cycle and promoting tumor growth (11). Exposure to cytotoxic drugs, inflammatory processes, ionization, and cigarette smoking are predisposing factors for ROS production (11). Some genetic mutations, such as those in Ras and p53 tumor suppressor genes, are associated with ROS activation (12,13). Additionally, the tumor angiogenesis of gliomas is induced by ROS, upregulating epidermal growth factor (EGF) and platelet-derived growth factor (PDGF) expression (14). Moreover, mitochondrial ROS induce oxidative stress, resulting in DNA damage and apoptosis induction (15). However,

* Corresponding author. Email: drtsaiwenchuan@mail2000.com.tw

ROS is associated with the enhancement of endoplasmic reticulum (ER) stress transcription factors, which include activating transcription factor 4 (ATF4), X-Box binding protein 1 (XBP1), and ATF6, to stimulate autophagy and angiogenesis in human cancers (16). However, Feng *et al* (17) demonstrated that PLP2 suppression could induce ER stress and autophagy and cause GBM apoptosis. Although the roles of ER stress and autophagy remain uncertain, PLP2 overexpression is considered oncogenic and results in aggressive glioma behavior (18).

In the present study, we first evaluated the relationship between A3C expression and common oncogenic factors in The Cancer Genome Atlas (TCGA) and Chinese Glioma Genome Atlas (CGGA) databases. In addition, IHC of human tissue microarrays was performed to confirm that A3C expression was not only related to tumor grades but also positively correlated with the overall survival time of various grades of gliomas. Finally, the correlation of the A3C and PLP2 IHC scores with glioma prognosis was performed to determine whether the combination of these biomarkers provided clinicians with stronger evidence than either of the biomarkers alone to predict the survival time of glioma patients.

Materials and Methods

In silico study

All clinical parameters and genomic data were collected from the TCGA database on the following websites: <https://xenabrowser.net/heatmap/>. The comparability of A3C with IDH-1 and EGF receptor (EGFR) mutations, phosphatase and tensin homolog (PTEN) expression, MGMT methylation, 1p/19q chromosomal co-deletion, and chromosomes 7 and 10 copy numbers was performed using the TCGA database.

Human glioma cell lines and Western blotting

Human glioma cell lines, A172, GBM8401, HS683, LN229, LN2308, T98G, U87, and U118, were purchased from the Cell Resource Center, Shanghai Institute of Biochemistry and Cell Biology at the Chinese Academy of Sciences (Shanghai, China). The cell lines were maintained in Dulbecco's modified Eagle medium comprising 13.1 mM NaHCO₃, 13 mM glucose, 2 mM glutamine, 10% fetal bovine serum, 100 U/mL penicillin, and 100 mg/mL streptomycin. The cell culture was incubated in a humidified incubator and supplied with 5% CO₂ at 37 °C. After the incubation period, lysis buffer, containing 10 mM Tris-HCl, 1 mM EGTA, 1 mM MgCl₂, 1 mM sodium orthovanadate, 1 mM DTT, 0.1% mercaptoethanol, 0.5% Triton X-100, and protease inhibitor cocktails, was added to the culture to lyse the cells. Cell lysates were prepared using 3 × 10⁷ cells from the mentioned glioma cell lines. Human normal brain tissue lysate (GeneTex, Inc., Irvine CA) was used as the control. Lysates were used for western blot analysis of A3C, with GAPDH (Santa Cruz Biotechnology, Texas, USA) as an internal control. The monoclonal mouse anti-β-actin antibody (Sigma-Aldrich, St. Louis, MO, USA) was employed as the primary antibody in western blotting. The analysis was performed according to a previously described protocol (19).

RNA isolation and real-time reverse transcription-PCR

Total RNA was extracted using the PAXGene™

Blood RNA kit (PreAnalytix), and the residual genomic DNA was digested using the RNase-Free DNase set (Qiagen, Hilden, Germany). Single-stranded cDNA was prepared from 1 g of the total RNA using a ThermoScript RT-PCR system (Invitrogen, Carlsbad, CA, USA). The mRNA expressions of selected genes were quantified via qRT-PCR. In addition, the human adult normal brain tissue cDNA (BioChain Institute, CA, USA) was used as the control. PCR was performed on a LightCycler™ instrument using the Fast-Start™ DNA Master SYBR Green I Real-Time PCR Kit (Thermo Fisher Scientific, MA, USA). Thermocycling was performed with a final volume of 20 μL of 3 mM magnesium chloride (MgCl₂), 0.5 μM of each of the required primers, and 10 μL of appropriately diluted cDNA. PCR was performed with an initial denaturation step of 10 min at 95 °C, followed by 40 cycles of a touch-down PCR protocol (10 s at 95 °C, 10 s annealing at 68–58 °C, and 16 s extension at 72 °C). Specific primers for GAPDH and PLP2 (see list below) were purchased from Search-LC (Heidelberg, Germany). To confirm amplification specificity, the PCR products from each of the primer pairs were subjected to a temperature of 58–98 °C (0.1 °C/s) for melting curve analysis.

Mouse GAPDH: 5'- GCACCGTCAAGGCTGAGAAC -3' (forward)

Mouse GAPDH: 5'- ATGGTGGTGAAGACGCCAGT -3' (reverse)

Mouse A3C: 5'- CTAAGAGGCTGAACATGAATC -3' (forward)

Mouse A3C: 5'- GGCTAGAGGAGACAGACCATG -3' (reverse)

Tissue microarray construction

Two sets of tissue microarray (no. GL2083a and GL2083b) were obtained from GenDiscovery Biotechnology Inc. After reviewing all microscopic images, we excluded the cases with incomplete tissue cores and incompatible diagnoses. From both microarrays, we included 76 gliomas and 5 non-neoplastic brain tissues in this study. Histological diagnosis by tissue microarrays depends on the 2016 WHO Classification of Tumors of the Central Nervous System. We used antigen retrieval and IHC staining of several biomarkers to explore the relationship between A3C expression and some well-known oncogenic factors. We utilized a monoclonal mouse anti-human IDH1 R132H antibody (1:100, Dianova, Hamburg, Germany), polyclonal rabbit anti-human ATRX antibody (1:100, ATLAS, Stockholm, Sweden), polyclonal rabbit anti-human Histone H3, mutant K27M (H3K27M) antibody (1:100, Millipore, Bedford, CA, USA), polyclonal rabbit anti-human Trimethyl-Histone H3, Lys27 (H3K27me3) antibody (1:1000, Millipore, Bedford, CA, USA), monoclonal mouse anti-human EGFR antibody (1:100, Thermo Fisher Scientific, San Jose, CA, USA), monoclonal mouse anti-human EGFRvIII antibody (1:100, Absolute, Oxford, UK), polyclonal rabbit anti-human AXL antibody (1:50, Sigma-Aldrich, St. Louis, MO, USA), monoclonal mouse anti-human phosphor-Axl (Y779) antibody (1:50, R&D system, Minneapolis, MN, USA), monoclonal mouse anti-human p53 antibody (1:100, DAKO, Carpinteria, CA, USA), monoclonal mouse anti-human neurofilament antibody (1:100, DAKO, Carpinteria, CA, USA), monoclonal mouse anti-human platelet-derived growth factor-α (PDGFRA) antibody (1:100, Santa Cruz Biotechnology,

Santa Cruz, TX, USA), polyclonal rabbit anti-human neurofibromin (NF1) antibody (1:100, Abcam, Cambridge, UK), and polyclonal rabbit anti-human nuclear receptor 77 (NUR77) antibody (1:100, Abcam, Cambridge, UK).

IHC analysis

The tissue microarray sections were dewaxed using xylene, rehydrated in alcohol, and immersed in 3% hydrogen peroxide for 5 min. Antigen retrieval was performed by heating the tissue sections (at 100 °C) for 30 min in 0.01 M sodium citrate buffer (pH 6.0). After three washes with phosphate-buffered saline (PBS), the tissue sections were incubated for 1 h at room temperature with a polyclonal rabbit anti-human A3C antibody (1:100, Thermo Fisher Scientific, MA, USA) and polyclonal rabbit anti-human PLP2 antibody (1:100, Biorbyt, Cambridge, UK) diluted in PBS. After three washes (5 min each in PBS), the tissue sections were incubated with biotin-labeled secondary immunoglobulin (1:100, DAKO, Glostrup, Denmark) for 1 h at room temperature. After three additional washes, peroxidase activity was assessed using a 3-amino-9-ethyl-carbazole chromogenic substrate (DAKO, Glostrup, Denmark) at room temperature. The IHC scores for A3C and PLP2 were calculated as the intensity of cytoplasmic and nuclear staining multiplied by the percentage of positively stained areas. Tissue microarray slides showed uniform staining, as observed in the original paraffin-embedded specimens. The intensities of A3C and PLP2 staining were scored on a scale previously described as follows: 0 (absence of staining), 1+ (weak staining), 2+ (moderate staining), and 3+ (strong staining).^[19] Tissues with less than 5% of tumor cells showing cytoplasmic or nuclear staining were considered to be IHC negative. To minimize technical bias, IHC staining for A3C and PLP2 was performed twice. The average of the two immunostaining scores for A3C and PLP2 represented the degree of expression of these biomarkers. Pancreatic ductal adenocarcinoma and human cerebellar tissues were used as positive controls for A3C and PLP2 expression, respectively.

Statistical analysis

The Pearson product-moment correlation test was performed to evaluate the relationship between the A3C immunostaining scores and glioma tumor grades. In addition, a Student’s *t*-test and one-way ANOVA were performed to evaluate the differences in A3C expression in each glioma subtype. Finally, survival time was calculated from the date of diagnosis to the date of death. Sixty-six patients with glioma, with 5 years of follow-up, were divided into four groups based on a set A3C and PLP2 immunostaining cut-off score. Statistical analysis of the overall survival time was performed using the Kaplan–Meier survival estimate. Furthermore, the independent prognostic factors in gliomas were evaluated by multivariate analysis.

Results

Expression of A3C correlated with advanced tumor grades and poor prognostic factors in the TCGA database

Higher A3C mRNA expression in primary and recurrent GBM was identified in the TCGA database compared to that in secondary GBM (Fig. 1). GBM is classified into classical, proneural, and mesenchymal subtypes based on

genome-wide transcriptome findings. Our results showed that the mesenchymal subtype of GBM had significantly higher A3C expression than the other two subtypes (Fig. 1). Additionally, A3C mRNA expression was inversely correlated with IDH1 mutations and MGMT methylation (Fig. 1). To evaluate the difference in A3C expression between non-tumor brain tissue and GBM, TCGA database showed significantly high mRNA expression in the highest-grade gliomas. G-CIMP is a prognostic factor associated with IDH mutations (20), therefore, high A3C expression was observed in the cases of GBM with non-G-CIMP and represented a poor prognosis. A heatmap of the TCGA database revealed that A3C expression tended to increase in chromosome 7 and decrease in chromosome 10, EGFR overexpression, and PTEN suppression.

High A3C mRNA and protein expression in GBM cell lines

To confirm the role of A3C in gliomas, we compared A3C protein expression in normal brain cell lysates and GBM cell lines. We found that most of the GBM cell lines, including A172, GBM8401, HS683, LN229, LNZ308, T98G, U87, and U118, had a higher A3C expression than normal cell lysates (Fig. 2A). Similar to A3C protein expression, A3C mRNA expression in the normal brain was lower than that in the GBM cell lines (Fig. 2B). Therefore, A3C appears to be a critical factor in the development of

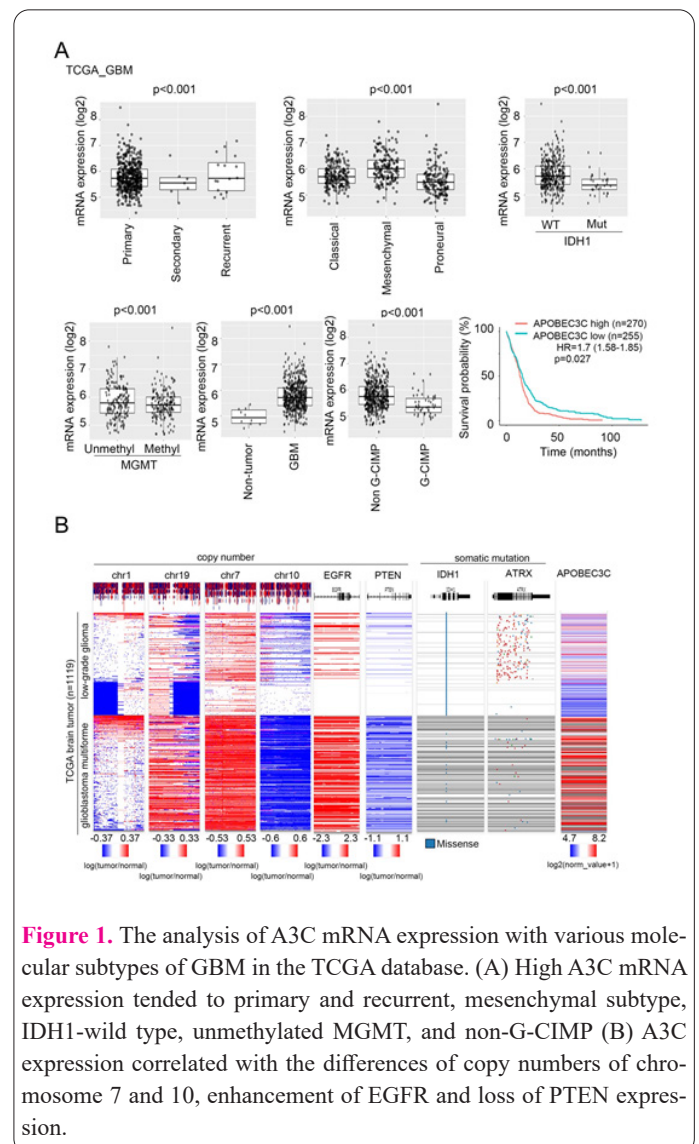


Figure 1. The analysis of A3C mRNA expression with various molecular subtypes of GBM in the TCGA database. (A) High A3C mRNA expression tended to primary and recurrent, mesenchymal subtype, IDH1-wild type, unmethylated MGMT, and non-G-CIMP (B) A3C expression correlated with the differences of copy numbers of chromosome 7 and 10, enhancement of EGFR and loss of PTEN expression.

Table 2. Univariate and multivariate analysis of risk factors associated with a positive A3C expression.

Variable	Univariate analysis		Multivariate analysis	
	OR (95% CI)	P value	OR (95% CI)	P value
Sex				
Male	1			
Female	0.75 (0.74-0.76)	0.087	0.76 (0.76-0.77)	0.395
Mutated				
IDH1 R132H				
Negative	1			
Positive	1.40 (1.04-2.71)	0.005*	1.46 (1.08-3.03)	0.008*
ATRX				
Preserve	1			
Loss	1.21 (1.19-1.24)	0.256	0.96 (0.94-0.97)	0.199
H3K27M				
Negative	1			
Positive	0.84 (0.72-1.12)	0.460	0.98 (0.89-1.10)	0.076
MGMT				
Negative	1			
Positive	0.70 (0.55-0.76)	0.037 [#]	0.68 (0.58-0.75)	0.003*
EGFR				
Positive	1			
Negative	0.53 (0.47-0.62)	0.006 [#]	0.56 (0.49-0.67)	0.166
EGFRvIII				
Positive	1			
Negative	0.46 (0.44-0.47)	<0.001 [#]	0.74 (0.72-0.77)	<0.001*
P53				
Overexpression	1			
Negative	0.67 (0.60-0.72)	0.018 [#]	0.69 (0.60-0.74)	0.005*
p-AxL				
Positive	1			
Negative	0.54 (0.29-0.72)	0.009 [#]	0.57 (0.31-0.75)	0.006*
NUR77				
Positive	1			
Negative	0.64 (0.50-0.74)	0.015 [#]	0.61 (0.46-0.71)	0.047*
PDGFRA				
Positive	1			
Negative	0.78 (0.61-1.28)	0.391	0.68 (0.54-1.06)	0.591

* The differences were analyzed by Pearson Correlation Method.

of A3C expression had a prognostic impact. To ensure an equal number of patients with high A3C (A3C-H) and low A3C (A3C-L) gliomas, the cut-off value of the A3C immunostaining score was set at 40. Subsequently, we performed a Kaplan–Meier analysis to evaluate the difference in the survival time between the two groups. Our results showed that the A3C-H group of gliomas had a higher percentage of shorter survival times than the A3C-L group (Fig. 4, $P = 0.039$). The multivariate analysis revealed that age, A3C expression, presence of the wild type-IDH1, loss of ATRX nuclear staining, phosphorylated AxL (p-AxL) overexpression, and PDGFRA overexpression were associated with poor prognosis in human gliomas (Table 3). Therefore, we demonstrated that the enhancement of A3C expression aids in the prognosis of patients with glioma.

Concordance of A3C and PLP2 protein expression has a more precise prognosis in gliomas

As A3C and PLP2 expressions were associated with the activation of oxidative stress, the comparative immunostaining scores of the above biomarkers were evaluated to determine their relationship. In this study, the statistical significance of A3C and PLP2 IHC expression was analyzed via linear regression analysis ($r = 0.343$) (Fig. 5A). Furthermore, gliomas with A3C-L and PLP2-L had a better prognosis than other groups of glial neoplasms ($P = 0.018$) (Fig. 5B). Therefore, the above findings imply an association between A3C and PLP2 protein expression, resulting in a short survival time of gliomas. However, the detailed mechanisms of action of A3C and PLP2 remain undetermined.

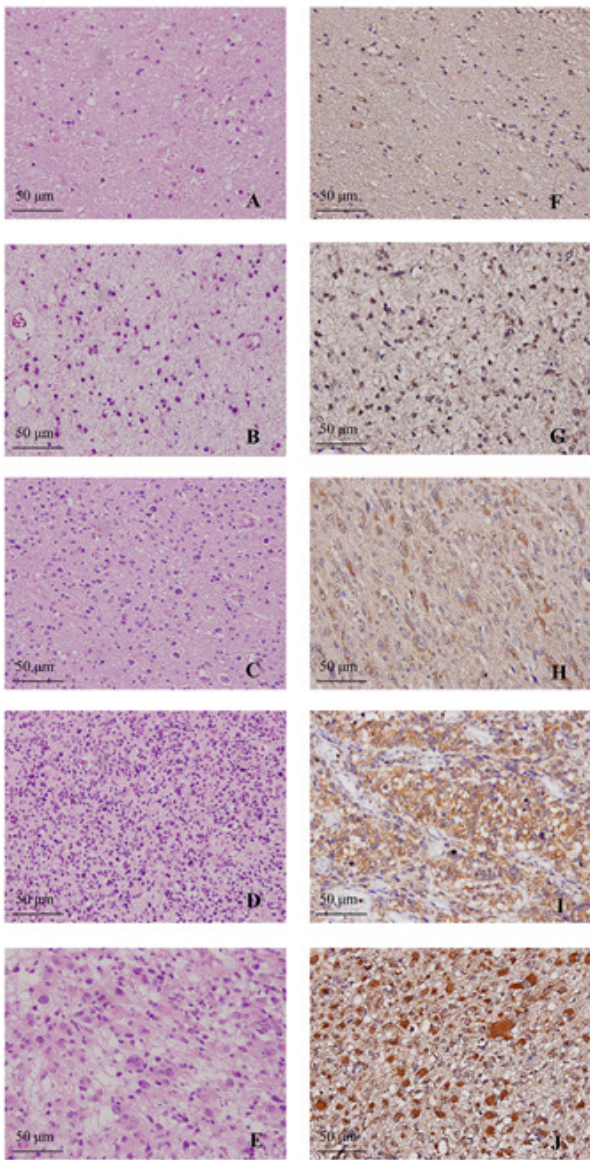


Figure 3. Representative hematoxylin and eosin staining of (A) non-neoplastic brain tissue, (B) pilocytic astrocytoma, (C) diffuse astrocytoma, (D) anaplastic astrocytoma, and (E) GBM; and representative immunohistochemical staining of A3C in (F) non-neoplastic brain tissue, (G) pilocytic astrocytoma, (H) diffuse astrocytoma, (I) 10 anaplastic astrocytoma, and (J) GBM (J). (Original magnification 400x).

Discussion

The APOBEC protein family comprises five members in the human genome: *APOBEC1*, *APOBEC2*, *APOBEC3*, *APOBEC4*, and activation-induced cytidine deaminase (*AICDA*) (21). *APOBEC3A* (A3A), *APOBEC3B* (A3B), A3C, *APOBEC3D* (A3D), *APOBEC3F* (A3F), and *APOBEC3G* (A3G) are distributed on chromosome 22 (22). Previous studies have revealed that the APOBEC family catalyzes cytosine deamination from single-stranded DNA to form uracil in human cancers (10). A3G, an Human immunodeficiency virus 1 restriction factor, targets double-stranded DNA and promotes DNA damage repair, potentially resulting in therapeutic resistance in human lymphoma cells (23,24). In addition, the upregulation of A3A can induce a DNA damage response and result in cell cycle arrest (24). Recent studies have demonstrated that high A3C mRNA expression is correlated with better clinical

outcomes in breast cancer and enhances the cytotoxic effects of cancer therapy (21,25). However, A3C expression is associated with advanced tumor grades and high IC50 values for chemotherapeutic regimens in low-grade gliomas (10). In the present study, we demonstrated that A3C is a neoplastic factor in tumor development through its association with the expression of well-known poor prognostic factors in gliomas.

A previous study demonstrated that PLP2 overexpression induces aggressive glioma behaviors, such as tumor proliferation, migration, invasion, and angiogenesis, by activating the phosphoinositide 3-kinase (PI3k)/mammalian target of rapamycin (mTOR)/ protein kinase B (AKT) and MAPK/ERK signaling pathways (18). In addition, the inhibition of PLP2 induces the cleavage of PARP-1 and the loss of DNA repair activity (26). Because the enhancement of PARP-1 depends on single-stranded DNA breaks resulting from ROS (27), PLP2 overexpression is likely associated with ROS activation. Additionally, the upregulation of A3C was strongly associated with cytochrome c oxidase (COX) family expression, particularly that of COX5A, COX5B, COX6A1, and COX6B1, based on the protein-protein interaction map. These COX members mentioned are involved in mitochondrial ROS activation or regulation under normoxia or hypoxia (28). As A3C was positively correlated with PLP2 expression, we inferred that both play important roles in upregulating ROS-induced cellular stress and further oncogenesis of gliomas. However, no adequate results have confirmed the relationship between A3C and PLP2, and further evidence is

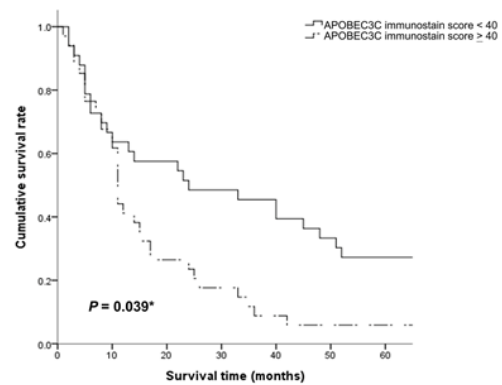


Figure 4. The correlation of A3C expression with prognosis in human gliomas by Kaplan-Meier analysis. ($P < 0.05$ means statistical significance).

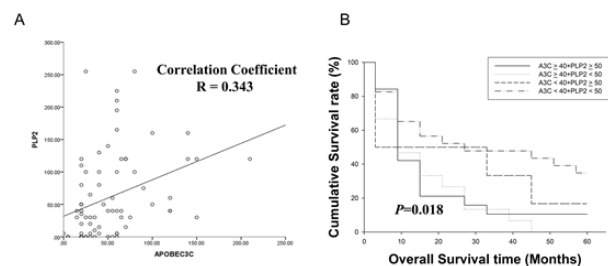


Figure 5. (A) Linear regression analysis of A3C and PLP2 immunostain scores in 62 gliomas. (B) Co-expression of A3C and PLP2 correlating with overall survival time in gliomas. Survival rates were analyzed using the Kaplan-Meier survival test.

Table 3. Multivariate Analysis for Overall Survival in gliomas.

Variable	Multivariate analysis		
	Hazard ratio	95% Coinfidence Interval	P value
Sex (male/female)	1.62	0.78-3.36	0.199
Age (<50/≥50)	3.81	1.64-8.89	0.002*
A3C (<40/≥40)	1.00	0.98-1.01	0.035*
IDH1 R132H (Wild type/Mutated)	2.65	1.02-6.91	0.046*
ATRX (Preserve/Loss)	0.40	0.19-0.85	0.018*
H3K27M (Negative/Positive)	0.86	0.28-2.63	0.796
MGMT (Unmethylated/ Methylated)	0.70	0.34-1.41	0.316
EGFR (Negative/Positive)	1.36	0.31-5.92	0.684
EGFRvIII (Negative/Positive)	1.58	0.51-4.94	0.432
P53 (Negative/Overexpression)	1.51	0.72-3.19	0.279
p-AxL (Negative/Positive)	4.17	1.57-11.06	0.004*
NUR77 (Negative/Positive)	0.53	0.25-1.11	0.090
PDGFRA (Negative/Positive)	11.81	1.75-80.00	0.011*

* The differences were analyzed by Pearson Correlation Method.

needed to elucidate the detailed mechanism. Compared to the Kaplan–Meier analysis of single A3C immunostaining scores, the combination of PLP2 and A3C IHC staining revealed a more significant correlation with glioma prognosis. Out of the four groups, with various immunostaining scores, A3C-L IHC staining predicted a relatively better survival rate than the A3C-H groups of gliomas, regardless of PLP2-L or PLP2-H. In our opinion, A3C and PLP2 IHC staining is a good tool for the accurate prognosis of gliomas based on WHO grades or molecular signatures.

In a previous study, A3C expression was associated with the mutated state of some well-known oncological factors of gliomas, including IDH1 R132H, MGMT, EGFRvIII, p53, p-AxL, and Nur77. The IDH1 R132H mutation comprises more than 90% of mutated-IDH1 gliomas and represents a better prognosis and a prolonged GBM development time in low-grade gliomas (29,30). TP53 loss-of-function and ATRX inactivation are strongly correlated with the IDH1 R132H mutation (31). MGMT methylation is a good predictor of response to TMZ treatment (32,33). Several studies have revealed that evaluating both MGMT protein expression and promoter methylation status is important for assessing the therapeutic efficacy of gliomas (34-36). As mismatch repair (MMR) proteins are responsible for DNA repair (37,38), the combination of low MGMT protein expression and MMR deficiency is the optimal prediction strategy for a good clinical outcome (39). In contrast, EGFRvIII overexpression indicates aggressive glioma behavior, including decreased tumor apoptosis and increased tumor progression (40). Recently, EGFRvIII-positive GBM cells showed the suppression of cell cycle checkpoint protein expression, including that of cyclin-dependent kinase 4 and mouse double minute 2 homolog (41). AxL belongs to the receptor tyrosine kinase family and is a poor prognostic factor in GBM (42). In addition, AxL induces tumor-associated macrophages and mediates tumor survival via interactions with growth arrest-specific protein 6 (43). p-AxL activates the PI3k/Akt cascade signaling pathway and further protects tumors from apoptosis (44). AxL prevented DNA damage-induced apoptosis in head and neck squamous cell carcinomas (45,46). Similar to A3C, most of the above oncological factors are

capable of inducing chemoresistance by repairing DNA breaks after TMZ treatment. Although the interaction between A3C and these factors is not clear, the application of A3C IHC might provide some useful information to clinicians about predicting therapeutic efficacy.

Conclusions

The current study demonstrated that A3C not only plays a role in tumorigenesis but also presents a poor prognosis for gliomas. A3C has been discovered as an oncological factor in gliomas based on the results of some databases and *in vitro* studies. Furthermore, we established that A3C protein expression may be associated with PLP2 in human glioma tissues; however, the mechanism is not clear. Additionally, our results indicate that the combination of A3C and aberrant gene expression is a good predictor of TMZ treatment outcome. In the future, pharmacological inhibitors of A3C may be beneficial for suppressing tumor progression and combating chemoresistance in gliomas.

Abbreviations

A3C: apolipoprotein B mRNA-editing enzyme catalytic polypeptide-like 3C; GBM: glioblastoma; IHC: immunohistochemical stain; IDH1: Isocitrate dehydrogenase 1; PLP2: proteolipid protein 2; ROS: reactive oxygen species; CNS: central nervous system; WHO: World Health Organization; ATRX: alpha-thalassemia x-linked mental retardation; MAPK/ERK: mitogen-activated protein kinase/extracellular signal-related kinase; RB: retinoblastoma; TMZ: temozolomide; MGMT: O⁶-methylguanine-DNA methyltransferase; PARP-1: poly [ADP-ribose] polymerase 1; EGF: epidermal growth factor; PDGF: platelet-derived growth factor; ER: endoplasmic reticulum; ATF4: activating transcription factor 4; XBP1: X-Box binding protein 1; TCGA: The Cancer Genome Atlas; CGGA: Chinese Glioma Genome Atlas; REMBRANDT: Repository of Molecular Brain Neoplasia Data; EGFR: EGF receptor; PTEN: phosphatase and tensin homolog; G-CIMP: glioma CpG island methylator phenotype; NUR77: nuclear receptor 77; H3K27M: Histone H3, mutant K27M; H3K27me3: Trimethyl-Histone H3, Lys27; PDGFRA: platelet-derived growth factor-alpha; NF1: neurofibro-

min; A3A: APOBEC3A; A3B: APOBEC3B; A3D: APOBEC3D; A3F: APOBEC3F; A3G: APOBEC3G; PI3k: phosphoinositide 3-kinase; mTOR: mammalian target of rapamycin; AKT: protein kinase B; COX: cytochrome c oxidase; MMR: mismatch repair;

Ethics approval and consent to participate

The patient tissue microarray study was approved by the Institutional Review Board, Tri-Service General Hospital, National Defense Medical Center (approval number: 1-108-05-154).

Acknowledgements

This study was supported by grants from the Tri-Service General Hospital, TSGH-E-111225, TSGH-E-112223, and National Defense Medical Center, MND-MAB-D-111115, and Ministry of Science and Technology, MOST 110-2320-B-016-008-MY3, Taiwan.

Interest conflict

There are no conflicts of interest.

References

- Goodenberger ML, Jenkins RB. Genetics of adult glioma. *Cancer Genet* 2012; 205: 613-21.
- Jäkel S, Dimou L. Glial Cells and Their Function in the Adult Brain: A Journey through the History of Their Ablation. *Front Cell Neurosci* 2017; 11: 24.
- Siegel RL, Miller KD, Fuchs HE, Jemal A. Cancer Statistics, 2021. *CA Cancer J Clin* 2021; 71: 7-33.
- Louis DN, Ohgaki H, Wiestler OD, Cavenee WK. WHO Classification of Tumours of the Central Nervous System. Lyon: IARC Press, 2016, pp. 16–122.
- Yang Z, Ling F, Ruan S, Hu J, Tang M, Sun X, et al. Clinical and Prognostic Implications of 1p/19q, IDH, BRAF, MGMT Promoter, and TERT Promoter Alterations, and Expression of Ki-67 and p53 in Human Gliomas. *Cancer Manag Res* 2021; 13: 8755-65.
- Olar A, Aldape KD. Using the molecular classification of glioblastoma to inform personalized treatment. *J Pathol* 2014; 232: 165-77.
- Stupp R, Mason WP, van den Bent MJ, Weller M, Fisher B, Taphoorn MJ, et al. Radiotherapy plus concomitant and adjuvant temozolomide for glioblastoma. *N Engl J Med* 2005; 352: 987-96.
- Higuchi F, Nagashima H, Ning J, Koerner MVA, Wakimoto H, Cahill DP. Restoration of Temozolomide Sensitivity by PARP Inhibitors in Mismatch Repair Deficient Glioblastoma is Independent of Base Excision Repair. *Clin Cancer Res* 2020; 26: 1690-9.
- Constantin D, Dubuis G, Conde-Rubio MDC, Widmann C. APOBEC3C, a nucleolar protein induced by genotoxins, is excluded from DNA damage sites. *FEBS J* 2022; 289: 808-31.
- Luo C, Wang S, Liao W, Zhang S, Xu N, Xie W, et al. Upregulation of the APOBEC3 Family Is Associated with a Poor Prognosis and Influences Treatment Response to Raf Inhibitors in Low Grade Glioma. *Int J Mol Sci* 2021; 22: 10390.
- Dröge W. Free radicals in the physiological control of cell function. *Physiol Rev* 2002; 82: 47-95.
- Tudek B, Winczura A, Janik J, Siomek A, Foksinski M, Oliński R. Involvement of oxidatively damaged DNA and repair in cancer development and aging. *Am J Transl Res* 2010; 2: 254-84.
- Yin, S.; van Meir, E.G. p53 Pathway Alterations in Brain Tumors. In *CNS Cancer: Models, Markers, Prognostic Factors, Targets and Therapeutic Approaches*; van Meir, E.G., Ed.; Humana Press (Springer): New York, NY, USA, 2009; pp. 283–314.
- Schieber M, Chandel NS. ROS function in redox signaling and oxidative stress. *Curr Biol* 2014; 24: R453-62.
- Valko M, Leibfritz D, Moncol J, Cronin MT, Mazur M, Telser J. Free radicals and antioxidants in normal physiological functions and human disease. *Int J Biochem Cell Biol* 2007; 39: 44-84.
- Paridaens A, Laukens D, Vandewynckel YP, Coulon S, Van Vlierberghe H, Geerts A, et al. Endoplasmic reticulum stress and angiogenesis: is there an interaction between them? *Liver Int* 2014; 34: e10-8.
- Feng Z, Zhou W, Wang J, Qi Q, Han M, Kong Y, et al. Reduced expression of proteolipid protein 2 increases ER stress-induced apoptosis and autophagy in glioblastoma. *J Cell Mol Med* 2020; 24: 2847-56.
- Chen YH, Hueng DY, Tsai WC. Proteolipid Protein 2 Overexpression Indicates Aggressive Tumor Behavior and Adverse Prognosis in Human Gliomas. *Int J Mol Sci* 2018; 19: 3353.
- Tsai, WC, Hueng, DY, Lin, CR, Yang, TC, Gao, HW. Nrf2 expressions correlate with WHO grades in gliomas and meningiomas. *Int J Mol Sci* 2016; 17: pii: E722.
- Malta TM, de Souza CF, Sabedot TS, Silva TC, Mosella MS, Kalkanis SN, et al. Glioma CpG island methylator phenotype (G-CIMP): biological and clinical implications. *Neuro Oncol* 2018; 20: 608-20.
- Zhang Y, Delahanty R, Guo X, Zheng W, Long J. Integrative genomic analysis reveals functional diversification of APOBEC gene family in breast cancer. *Hum Genomics* 2015; 9: 34.
- Jarmuz A, Chester A, Bayliss J, Gisbourne J, Dunham I, Scott J, et al. An anthropoid-specific locus of orphan C to U RNA-editing enzymes on chromosome 22. *Genomics* 2002; 79: 285-96.
- Harris RS, Petersen-Mahrt SK, Neuberger MS. RNA editing enzyme APOBEC1 and some of its homologs can act as DNA mutators. *Mol Cell* 2002; 10: 1247-53.
- Kan Z, Jaiswal BS, Stinson J, Janakiraman V, Bhatt D, Stern HM, et al. Diverse somatic mutation patterns and pathway alterations in human cancers. *Nature* 2010; 466: 869-73.
- Tao L, Jiang Z, Xu M, Xu T, Liu Y. Induction of APOBEC3C Facilitates the Genotoxic Stress-Mediated Cytotoxicity of Artesunate. *Chem Res Toxicol* 2019; 32: 2526-37.
- Maia VSC, Berzaghi R, Arruda DC, Machado FC, Loureiro LL, Melo PMS, et al. PLP2-derived peptide Rb4 triggers PARP-1-mediated necrotic death in murine melanoma cells. *Sci Rep* 2022; 12: 2890.
- Jankevicius G, Hassler M, Golia B, Rybin V, Zacharias M, Timinszky G, et al. A family of macrodomain proteins reverses cellular mono-ADP-ribosylation. *Nat Struct Mol Biol* 2013; 20: 508-14.
- Bourens M, Fontanesi F, Soto IC, Liu J, Barrientos A. Redox and reactive oxygen species regulation of mitochondrial cytochrome C oxidase biogenesis. *Antioxid Redox Signal* 2013; 19: 1940-52.
- Parsons DW, Jones S, Zhang X, Lin JC, Leary RJ, Angenendt P, et al. An integrated genomic analysis of human glioblastoma multiforme. *Science* 2008; 321: 1807-12.
- Leu S, von Felten S, Frank S, Boulay JL, Mariani L. IDH mutation is associated with higher risk of malignant transformation in low-grade glioma. *J Neurooncol* 2016; 127: 363-72.
- Núñez FJ, Mendez FM, Kadiyala P, Alghamri MS, Savelieff MG, Garcia-Fabiani MB, et al. IDH1-R132H acts as a tumor suppressor in glioma via epigenetic up-regulation of the DNA damage response. *Sci Transl Med* 2019; 11: eaaq1427.
- Weller M, Stupp R, Reifenberger G, Brandes AA, van den Bent MJ, Wick W, et al. MGMT promoter methylation in malignant

- gliomas: ready for personalized medicine? *Nat Rev Neurol* 2010; 6: 39-51.
33. Mansouri A, Hachem LD, Mansouri S, Nassiri F, Laperriere NJ, Xia D, *et al.* MGMT promoter methylation status testing to guide therapy for glioblastoma: refining the approach based on emerging evidence and current challenges. *Neuro Oncol* 2019; 21: 167-78.
 34. Mason S, McDonald K. MGMT testing for glioma in clinical laboratories: discordance with methylation analyses prevents the implementation of routine immunohistochemistry. *J Cancer Res Clin Oncol* 2012; 138: 1789-97.
 35. Pandith AA, Qasim I, Zahoor W, Shah P, Bhat AR, Sanadhya D, *et al.* Concordant association validates MGMT methylation and protein expression as favorable prognostic factors in glioma patients on alkylating chemotherapy (Temozolomide). *Sci Rep* 2018; 8: 6704.
 36. Karayan-Tapon L, Quillien V, Guilhot J, Wager M, Fromont G, Saikali S, *et al.* Prognostic value of O6-methylguanine-DNA methyltransferase status in glioblastoma patients, assessed by five different methods. *J Neurooncol* 2010; 97: 311-22.
 37. Wick W, Weller M, van den Bent M, Sanson M, Weiler M, von Deimling A, *et al.* MGMT testing--the challenges for biomarker-based glioma treatment. *Nat Rev Neurol* 2014; 10: 372-85.
 38. Thomas A, Tanaka M, Trepel J, Reinhold WC, Rajapakse VN, Pommier Y. Temozolomide in the Era of Precision Medicine. *Cancer Res* 2017; 77: 823-26.
 39. Butler M, Pongor L, Su YT, Xi L, Raffeld M, Quezado M, *et al.* MGMT Status as a Clinical Biomarker in Glioblastoma. *Trends Cancer* 2020; 6: 380-391.
 40. Gan HK, Cvrljevic AN, Johns TG. The epidermal growth factor receptor variant III (EGFRvIII): where wild things are altered. *FEBS J* 2013; 280: 5350-70.
 41. Hoogstrate Y, Ghisai SA, de Wit M, de Heer I, Draaisma K, van Riet J, *et al.* The EGFRvIII transcriptome in glioblastoma: A meta-omics analysis. *Neuro Oncol* 2022; 24: 429-441.
 42. Cheng P, Phillips E, Kim SH, Taylor D, Hielscher T, Puccio L, *et al.* Kinome-wide shRNA screen identifies the receptor tyrosine kinase AXL as a key regulator for mesenchymal glioblastoma stem-like cells. *Stem Cell Rep* 2015; 4: 899-913.
 43. Ben-Batalla I, Schultze A, Wroblewski M, Erdmann R, Heuser M, Waizenegger JS, *et al.* Axl, a prognostic and therapeutic target in acute myeloid leukemia mediates paracrine crosstalk of leukemia cells with bone marrow stroma. *Blood* 2013; 122: 2443-52.
 44. Varnum BC, Young C, Elliott G, Garcia A, Bartley TD, Fridell YW, *et al.* Axl receptor tyrosine kinase stimulated by the vitamin K-dependent protein encoded by growth-arrest-specific gene 6. *Nature* 1995; 373: 623-6.
 45. McDaniel NK, Iida M, Nickel KP, Longhurst CA, Fischbach SR, Rodems TS, *et al.* AXL Mediates Cetuximab and Radiation Resistance Through Tyrosine 821 and the c-ABL Kinase Pathway in Head and Neck Cancer. *Clin Cancer Res* 2020; 26: 4349-59.
 46. Hong J, Peng D, Chen Z, Sehdev V, Belkhir A. ABL regulation by AXL promotes cisplatin resistance in esophageal cancer. *Cancer Res* 2013; 73: 331-40.